DECIMATION OF FINITE-DIFFERENCE TIME-DOMAIN SCHEMES IN 1D AND 2D BOUNDARY-ABSORBING ACOUSTIC MODEL SIMULATIONS

M. Novello, F. Fontana, E. Bozzo

University of Udine
Department of Electric, Management and Mechanical Engineering
Department of Mathematics and Computer Science
Via delle Scienze 206, Udine 33100, Italy

ABSTRACT

A decimated version of a broad family of Finite-Difference Time-Domain schemes is derived by an algebraic rearrangement of their matrix formulation, allowing for computing the grid nodes at half the temporal steps compared to the original scheme. This rearrangement can ask for solving a generalized matrix inversion problem. The decimated scheme generates solutions having comparable accuracy to that exhibited by the original simulations. However, the broader applicability of the proposed technique requires to solve currently unanswered theoretical issues of spatial grid decimation, as well as to make extensive tests using large matrices.

Index Terms— Numerical wave propagation, Decimation, Multidimensional acoustic field modeling.

1. INTRODUCTION

Finite-Difference Time-Domain (FDTD) schemes are used to solve a variety of wave propagation problems especially in the electro-magnetics [1] and acoustics [2] fields. Besides some core numerical issues of stability and accuracy, that depend on the specific propagation problem and must be dealt with during the design of the FDTD model, further concerns arise at the simulation stage due to the computational resources that are needed by the resulting solver. Among such concerns, the simulation time turns out to be an important factor: even if in principle a longer simulation requires simply more CPU or GPU time, in practical terms every update of a large FDTD grid asks the machine to perform a huge computational effort, often resulting in exceedignly slow evolutions of the solution even in state-of-the-art hardware architectures [3].

Most musical instrument sounds and, in general, a lot of environmental sonic events resulting from the physical interaction between real objects—for instance, noisy impacts between colliding bodies—exhibit a peculiar evolution of the spectral energy [4]: this energy in fact is broadband in correspondence of the excitation and immediately after it has ceased; past this *attack transient*, the spectral components in the high frequency rapidly decay depending on the resonance and absorption properties of the acoustic object propagating the sound after the excitation. For this reason, if one models an acoustic scenario like this through the FDTD approach then the resulting scheme processes only a fraction of the available bandwidth as soon as the initial transient is over and the system steady state evolution is reached.

If we could adapt the computation step and the grid density at runtime to account for these changes in the bandwidth of the solution, then a considerable amount of computation time and memory could be saved when the solver is reproducing the steady sound. This idea has been recently exploited in the realization of digital filters, whose rate accommodates runtime changes of the signal bandwith [5]. In this paper we show that a broad family of second-order FDTD schemes, which finds application in multidimensional acoustic wave modeling with absorption, can be decimated in time if the frequency content of the sound waves is limited below half Nyquist.

Since a theoretical characterization of the FDTD decimation problem is actually in progress, the paper limits its scope to the formal derivation of the decimated scheme, and then to its comparison against the original via 1D and 2D simulations. Other important issues, in particular the spatial decimation of the FDTD grid holding the necessary conditions in the spectral content of the numerical waves, are part of the ongoing research work of the authors.

1.1. Relation to prior work

Research on efficient meanwhile accurate models describing the excitation and consequent sound production of an acoustic resonator, ranging from simple colliding bodies up to musical instruments, nowadays moves along three mainstream lines: modal synthesis [6, 7], spectral methods [8], and FDTD modeling. Particularly the third approach, which is object of this paper, has shown potential to describe complex scenarios [9]. With regard to these descriptions, much research has been done in an effort to reduce the computation time without sacrificing the simulation accuracy especially in the electro-

978-1-4799-2893-4/14/$31.00 ©2014 IEEE

magnetic transmission field [10, 1], but also with specific focus on efficient FDTD models of acoustic wave propagation across 3D domains with absorbing boundaries [11].

The idea of applying the well-established notion of decimation [12] directly onto the FDTD grid, i.e. not to the output signal as part of a post-processing procedure, seems yet to be explored: in this sense, our results complement the aforementioned research works on efficient FDTD modeling.

2. FDTD STRING AND MEMBRANE MODEL

Ideal 1D and 2D wave propagation across lossless isotropic media is usually simulated on a finite spatial-temporal grid by the following FDTD schemes:

$$u_i^{n+1} = \lambda^2(u_{i-1}^n + u_{i+1}^n) + 2(1-\lambda^2)u_i^n - u_i^{n-1} \tag{1}$$

for the vibrating string, and

$$\begin{aligned} u_{i,j}^{n+1} = &\lambda^2(u_{i-1,j}^n + u_{i+1,j}^n + u_{i,j-1}^n + u_{i,j+1}^n) \\ &+ 2(1-2\lambda^2)u_{i,j}^n - u_{i,j}^{n-1} \end{aligned} \tag{2}$$

for the vibrating membrane. The temporal step k, spatial step h and propagation velocity c of the wave signal u are embedded in the Courant parameter $\lambda = ch/k$. The coefficients n, i, and j denote the discrete point in time and space where u is computed respectively by (1) and (2). Such a computation must cover the whole spatial grid, i.e., the entire range for i and j, across the temporal steps of interest that are spanned by n. In practice the grid update needs proper initial and boundary conditions, respectively adding further temporal and spatial constraints to the edge nodes that, otherwise, could not be computed by (1) and (2).

The Courant parameter governs the stability of the FDTD scheme. For the purpose of this paper, it can be set to $\lambda = 1$ and $\lambda = 1/\sqrt{2}$ respectively for the string and the membrane model, resulting in schemes working at the stability limit.

Energy dissipation results in terms adding up to (1) and (2). A simple, however implicit scheme which considers a constant viscous damping parameter $\gamma \geq 0$ in the string takes the following form:

$$(1+\gamma\frac{k}{2})u_i^{n+1} = u_{i-1}^n + u_{i+1}^n - (1-\gamma\frac{k}{2})u_i^{n-1}. \tag{3}$$

Additionally, boundary absorption can be considered. If we model a *locally reacting surface*, then a reflection coefficient ρ can be figured out from the acoustic impedance of the transmission medium. This coefficient must be embedded in (1) and (2) in correspondence of the edge nodes. In practice it is $\rho \in [0,1]$, with $\rho = 0$ in the case of (Mur) total absorption, and $\rho = 1$ in the case of (typically Dirichlet or Neumann) total reflection. In between this range, frequency-dependent absorption boundaries can be modeled through the design of the reflection coefficient in terms of a linear transfer characteristic, whose realization is made through a digital filter [11].

The above models can be expressed using the following matrix notation:

$$\boldsymbol{C}\underline{u}^{n+1} = \boldsymbol{A}\underline{u}^n - \boldsymbol{B}\underline{u}^{n-1}, \tag{4}$$

in which $\underline{u}^n$ contains the numerical signal over all nodes at temporal step n. In more detail, this formula can describe second-order FDTD schemes made of M nodes, modeling viscous damping and first-order boundary absorption filters. Thus, $\boldsymbol{A}$, $\boldsymbol{B}$ and $\boldsymbol{C}$ are matrices sized $M \times M$.

In absence of viscosity it is $\boldsymbol{C} = \boldsymbol{I}$, furthermore $\boldsymbol{B} = \boldsymbol{I}$ if the boundaries reflect all the energy—$\boldsymbol{I}$ is the identity matrix. Hence, relation (4) simplifies in $\underline{u}^{n+1} = \boldsymbol{A}\underline{u}^n - \underline{u}^{n-1}$ in the lossless case. Furthermore, one can always explicit the term $\underline{u}^{n+1}$ provided the invertibility of $\boldsymbol{C}$ in presence of viscous damping. In the following we will assume to work with explicit FDTD schemes, so to elaborate on the relation

$$\underline{u}^{n+1} = \boldsymbol{A}\underline{u}^n - \boldsymbol{B}\underline{u}^{n-1}. \tag{5}$$

3. TEMPORAL DECIMATION

Given an explicit second-order FDTD scheme, we wonder whether it is possible to speed up the computations without loss of accuracy of the solution. By properly reworking relation (5) we will come up with a *temporal decimation* of the original FDTD scheme. Decimation cuts the computation of the output to half the samples otherwise computed by the original model: if $n = 1, 2, 3, 4, 5, \ldots$ are the original temporal steps, then the decimated scheme will compute only the steps $n_d = 1, 3, 5, \ldots$.

We consider three adjacent steps of computation:

$$\begin{cases} \underline{u}^n - \boldsymbol{A}\underline{u}^{n-1} + \boldsymbol{B}\underline{u}^{n-2} = 0 \\ \underline{u}^{n-1} - \boldsymbol{A}\underline{u}^{n-2} + \boldsymbol{B}\underline{u}^{n-3} = 0 \\ \underline{u}^{n-2} - \boldsymbol{A}\underline{u}^{n-3} + \boldsymbol{B}\underline{u}^{n-4} = 0 \end{cases}. \tag{6}$$

By multiplying the second equation by $\boldsymbol{A}$ and the third equation by a square matrix $\boldsymbol{M}$, we can eliminate the term $\underline{u}^{n-1}$ hence obtaining:

$$\begin{aligned} \underline{u}^n - &(\boldsymbol{A}^2 - \boldsymbol{B} - \boldsymbol{M})\underline{u}^{n-2} \\ &-(\boldsymbol{M}\boldsymbol{A} - \boldsymbol{A}\boldsymbol{B})\underline{u}^{n-3} + \boldsymbol{M}\boldsymbol{B}\underline{u}^{n-4} = 0. \end{aligned} \tag{7}$$

The cancellation of $\underline{u}^{n-3}$ in (7) depends on the solution of the matrix equation $\boldsymbol{M}\boldsymbol{A} = \boldsymbol{A}\boldsymbol{B}$ with respect to $\boldsymbol{M}$. In the lossless model it is $\boldsymbol{B} = \boldsymbol{I}$. For this model, and more in general when $\boldsymbol{A}$ and $\boldsymbol{B}$ commute, we can set $\boldsymbol{M} = \boldsymbol{B}$, then nullify the difference $\boldsymbol{M}\boldsymbol{A} - \boldsymbol{A}\boldsymbol{B} = \boldsymbol{B}\boldsymbol{A} - \boldsymbol{A}\boldsymbol{B}$ and finally make use of the scheme

$$\underline{u}^n = (\boldsymbol{A}^2 - 2\boldsymbol{B})\underline{u}^{n-2} - \boldsymbol{B}^2\underline{u}^{n-4}. \tag{8}$$

If there is boundary absorption then $\boldsymbol{A}$ and $\boldsymbol{B}$ do not necessarily commute; in this case, if $\boldsymbol{A}$ is non-singular then by setting $\boldsymbol{M} = \boldsymbol{A}\boldsymbol{B}\boldsymbol{A}^{-1}$ we can still eliminate the term $\underline{u}^{n-3}$: this is the case for e.g. an absorbing string model made of an even number of nodes.

Conversely, if this number is odd then $\boldsymbol{A}$ cannot be inverted. In fact, in this case the matrix defines a null space which is aligned with the vector

$$\{1, 0, -1, 0, 1, 0, \ldots, 0, \pm 1\},$$

representative of a spatial component located *exactly* at half Nyquist. In other words, an FDTD model of a string based on a grid having an odd number of nodes can represent the spatial component at half Nyquist, preventing from decimation. In this case we can resort to the Moore-Penrose *pseudo-inverse* $\boldsymbol{A}^\dagger$ [13]. By setting $\boldsymbol{M} = \boldsymbol{A}\boldsymbol{B}\boldsymbol{A}^\dagger$ in fact we get

$$\boldsymbol{A}\boldsymbol{B} - \boldsymbol{M}\boldsymbol{A} = \boldsymbol{A}\boldsymbol{B} - \boldsymbol{A}\boldsymbol{B}\boldsymbol{A}^\dagger\boldsymbol{A} = \boldsymbol{A}\boldsymbol{B}(\boldsymbol{I} - \boldsymbol{A}^\dagger\boldsymbol{A}).$$

Now, $\boldsymbol{I} - \boldsymbol{A}^\dagger\boldsymbol{A}$ is the orthogonal projection over the kernel of $\boldsymbol{A}$ [13]. If $\underline{u}^{n-3}$ is orthogonal to this kernel as well, then $(\boldsymbol{I} - \boldsymbol{A}^\dagger\boldsymbol{A})\underline{u}^{n-3} = 0$. The simulations appearing in the next section will suggest that orthogonality can be assumed to hold in practice. At this stage of the research we speculate that this kernel is made of spatial frequency components having a lower limit at half Nyquist: if this is true, then neglecting the term in $\underline{u}^{n-3}$ in (7) does not introduce any appreciable error in the computations once setting $\boldsymbol{M} = \boldsymbol{A}\boldsymbol{B}\boldsymbol{A}^\dagger$.

The case of the membrane presents analogous problems concerning the derivation of the decimated scheme in presence of an odd number of nodes in either direction. Again, if $\boldsymbol{A}$ cannot be inverted then the pseudo-inverse $\boldsymbol{A}^\dagger$ can be invoked. However, also in this case the simulations do not exhibit appreciable errors once the term in $\underline{u}^{n-3}$ is removed.

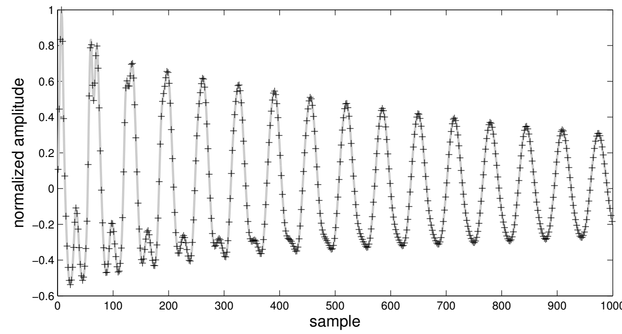

(a) Even-numbered grid (30 nodes). Raised cosine excitation on node 10. Pick-up point on node 2. Absorption: $R = 0.575$.

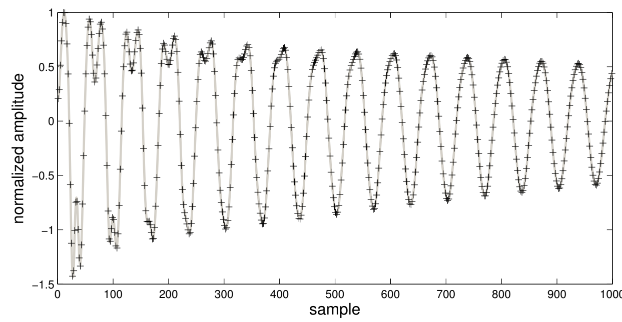

(b) Odd-numbered grid (31 nodes). Raised cosine excitation on node 20. Pick-up point on node 4. Absorption: $R = 0.575$.

Fig. 1. FDTD simulation of the string. Grey solid line: original scheme; Black crosses: decimated scheme. Largest positive value normalized to unity.

4. STRING AND MEMBRANE MODEL SIMULATIONS

This section illustrates results from FDTD simulations of simple string and membrane models, all obtained from a Pentium Dual Core laptop computer running Matlab. Both models include a frequency-dependent absorbing boundary, progressively canceling the higher frequencies in ways that the scheme can be eventually decimated at runtime. Boundary absorption is realized by introducing a parameter R in the equation governing the scheme in correspondence of the edge nodes:

$$u_i^{n+1} = \sum_j u_j^n - R u_i^{n-1}, \tag{9}$$

where j ranges over the indices of the nodes that are adjacent to the ith node in the spatial grid.

Furthermore, the initial condition $\underline{u}^0 = \underline{u}_0$ (i.e., on displacement) has been completed by setting the first derivative of $\underline{u}$ (i.e., the velocity) null at all nodes.

Figure 1 shows plots of the signal outcoming from an FDTD string model made of a spatial grid measuring an even and odd number of nodes, respectively above and below. Both schemes have been excited with a spatial raised cosine, minimizing the introduction of spectral energy above half Nyquist. In the odd number case, plots of both the absolute (lower solid line) and relative (lower dashed line) errors between the signal values in the original and decimated signal have been plotted in Figure 3 after normalization to unity of the outputs.

Figure 2 shows plots of the signal outcoming from an FDTD membrane model made of a spatial grid measuring an even and odd number of nodes, respectively above and below. Both schemes have been excited with a Gaussian function, containing spectral energy above half Nyquist. A switch to the decimated scheme has been performed after inspection of a spectrogram of the signal, once the energy of the lowest component above half Nyquist had decayed by 60 dB with respect to the component at the fundamental frequency. In the odd number case, plots of both the absolute (upper solid line) and relative (upper dashed line) errors between the signal values in the original and decimated signal have been plotted in Figure 3 past the switch to the decimated scheme, and after normalization to unity of the largest positive value of the sig-

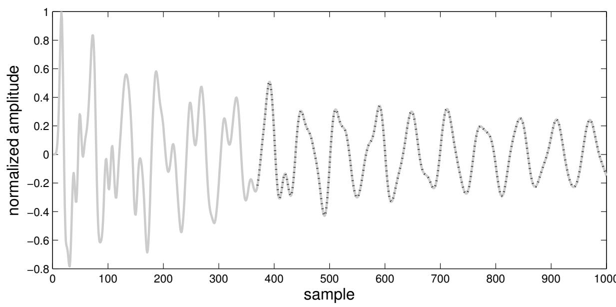

(a) Even-numbered grid, 30×30 nodes, center reference (0,0). Gaussian excitation on node (0,1), variance 2.5. Pick-up point on node 132. Switch at temporal step 350. Absorption: size $R = 0.7929$; corner $R = 0.5858$.

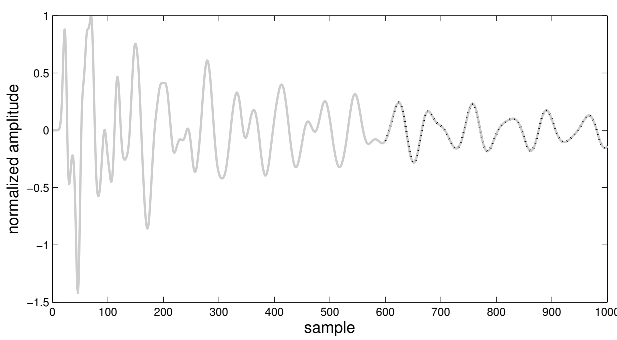

(b) Odd-numbered grid, 31×31 nodes, center reference (0,0). Gaussian excitation on node (-8,-1), variance 2.5. Pick-up point on node 365. Switch at temporal step 600. Absorption: size $R = 0.7271$; corner $R = 0.4541$.

Fig. 2. FDTD simulation of the membrane. Grey solid line: original scheme; Black dotted line: decimated scheme. Largest positive value normalized to unity.

nal.

5. FINAL REMARKS

We have shown that the decimated scheme has promising potential to follow the simulation of the original scheme with a high degree of accuracy. At least in our simulations, the differences between the original and decimated output signal were in fact negligible in both string and membrane models. In any case, some remarks must be pointed out before the conclusion.

First, even if the decimated scheme computes half temporal grid points, nevertheless the pseudo-inverse is typically a full matrix and calls for a solving procedure for (7) having a computational cost $O(M^2)$. Fortunately, due to the particular structure of $\boldsymbol{A}$, in the 1D case it is possible to reduce the computations in (7) to a complexity $O(M)$. Furthermore, in the 2D case the same complexity can be reduced to $O(M \log M)$ [14].

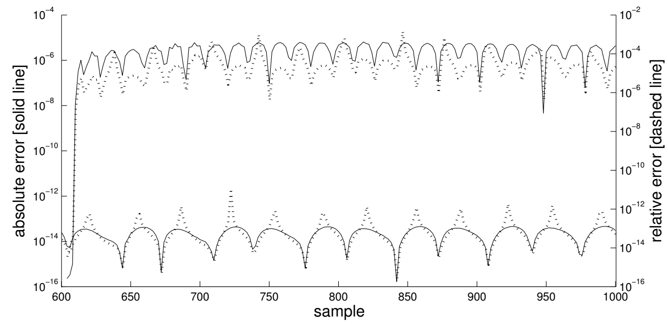

Fig. 3. Solid line: absolute error from (below) the string simulation of Fig. 1(b), and (above) the membrane simulation of Fig. 2(b). Dashed line: relative error from (below) the string simulation of Fig. 1(b), and (above) the membrane simulation of Fig. 2(b). Inspection starting from sample no. 600, i.e. after the switch to the decimated scheme occurring in the membrane simulation.

Second, the inversion problem must be tested in large matrices accounting for more realistic modeling of wave transmission and absorption.

Finally, a substantial boost to the proposed technique may come from the joint spatial and temporal (also iterated) decimation of the FDTD grid. If, intuitively, the domain grid can be pruned once the spatial frequency components occupy only the low range, on the other hand the rigorous treatment of this matter is not obvious especially in presence of dissipation in the model. The authors are dealing with this issue, as part of their current research in the topic.

6. REFERENCES

[1] D.M. Sullivan, *Electromagnetic simulation using the FDTD method*, Wiley-IEEE Press, 2013.

[2] Stefan Bilbao, "Optimized FDTD schemes for 3-D acoustic wave propagation," *IEEE Trans. on Audio, Speech and Language Processing*, vol. 20, no. 5, pp. 1658–1663, 2012.

[3] Craig J. Webb and Stefan Bilbao, "Computing room acoustics with CUDA-3D FDTD schemes with boundary losses and viscosity," in *Proc. Int. Conf. on Acoustics, Speech and Signal Processing (ICASSP)*, Prague, Czech Republic, May 2011, IEEE, pp. 317–320.

[4] D. Rocchesso, R. Bresin, and M. Fërnstrom, "Sounding objects," *IEEE Multimedia*, vol. 10, no. 2, 2003.

[5] F. Fontana, S. Zambon, and E. Bozzo, "Rate switching filters: Model and efficient approximation," *IEEE Trans. on Signal Processing*, vol. 62, no. 5, pp. 1290–1304, March 2014.

[6] F. Avanzini and R. Marogna, "A modular physically based approach to the sound synthesis of membrane percussion instruments," *IEEE Trans. on Audio, Speech and Language Processing*, vol. 18, no. 4, pp. 891–902, 2010.

[7] B. Bank, S. Zambon, and F. Fontana, "A modal-based real-time piano synthesizer," *IEEE Trans. on Audio, Speech and Language Processing*, vol. 18, no. 4, pp. 809–821, 2010, Special Issue on Virtual Analog Audio Effects and Musical Instruments.

[8] Nicolas Bonneel, George Drettakis, Nicolas Tsingos, Isabelle Viaud-Delmon, and Doug James, "Fast modal sounds with scalable frequency-domain synthesis," in *ACM SIGGRAPH 2008 papers*, New York, NY, USA, 2008, SIGGRAPH '08, pp. 24:1–24:9, ACM.

[9] S. Bilbao, "Modeling of complex geometries and boundary conditions in finite difference/finite volume time domain room acoustics simulation," *IEEE Trans. on Audio, Speech and Language Processing*, vol. 21, no. 7, pp. 1524–1533, 2013.

[10] Burkay Donderici and Fernando L Teixeira, "Improved FDTD subgridding algorithms via digital filtering and domain overriding," *IEEE Trans. on Antennas and Propagation*, vol. 53, no. 9, pp. 2938–2951, 2005.

[11] K. Kowalczyk and M. van Walstijn, "Room acoustics simulation using 3-D compact explicit FDTD schemes," *IEEE Trans. on Audio, Speech and Language Processing*, vol. 19, no. 1, pp. 34–46, 2011.

[12] S. K. Mitra, *Digital Signal Processing. A computer-Based Approach*, McGraw-Hill, New York, 1998.

[13] Adi Ben-Israel and Thomas N. E. Greville, *Generalized inverses*, CMS Books in Mathematics/Ouvrages de Mathématiques de la SMC, 15. Springer-Verlag, New York, second edition, 2003, Theory and applications.

[14] Paul N. Swarztrauber, "The methods of cyclic reduction, fourier analysis and the FACR algorithm for the discrete solution of Poisson's equation on a rectangle," *SIAM Review*, vol. 19, no. 3, pp. 490–501, 1977.